Size quantization of excitons and determination of the parameters of their energy spectrum in CuCl

A. I. Ekimov, A. A. Onushchenko, A. G. Plyukhin, and Al. L. Éfros

A. F. Ioffe Physicotechnical Institute, Academy of Sciences of the USSR, Leningrad

(Submitted 8 November 1984)
Zh. Eksp. Teor. Fiz. **88**, 1490–1501 (April 1985)

Optical spectroscopy methods were used to investigate the size quantization of the energy spectrum of excitons in CuCl microcrystals dispersed in a transparent dielectric matrix. The size of microcrystals grown by diffusion-type precipitation of a new phase in a supersaturated solid solution was deliberately varied from tens to thousands of angstroms. It was found that the profile of a luminescence line of free excitons was due to the dispersion of the size of microcrystals described by the Lifshitz–Slezov distribution for the recondensation stage of the growth of microcrystals. A theory of the size quantization of excitons allowing for the complex structure of the valence band was developed. A comparison with the experimental results yielded the energy band parameters describing the energy spectrum of excitons in a CuCl crystal.

I. INTRODUCTION

It has been recently demonstrated that ultradisperse semiconducting microcrystals can be grown inside a transparent dielectric matrix.[1] A method for the growth of microcrystals by a diffusion-type precipitation of a new phase of a supersaturated solid solution developed by Golubkov *et al.*[1] makes it possible to control the size of the resultant particles over a wide range from tens to thousands of angstroms. The silicate glass matrix is transparent in a wide range of wavelengths from ultraviolet to the near infrared part of the spectrum, so that it is possible to use optical spectroscopy methods for investigating the properties of microcrystals.

Heterophase systems of this kind represent a new class of objects for investigating various "size" effects in semiconductors and, in particular, the quantum size effect. In fact, a semiconducting microcrystal in a dielectric matrix represents a three-dimensional potential well of size which limits the region of motion of quasiparticles. Consequently, free motion of quasiparticles in a microcrystal is possible only for certain values of the energy and the energy spectrum in quantized.[2–4]

The problem of manifestation of the size quantization effect in the exciton and interband absorption spectra of spherical semiconducting microscrystals is considered theoretically in Ref. 5. It is shown that the influence of the quantum size effect on the absorption and luminescence spectra of microcrystals depends strongly on the ratio of the exciton radius a_{ex} to the microcrystal radius a. In the case when $a_{ex} \ll a$, an exciton is quantized as a whole and the influence of the boundaries of a microcrystal on the exciton binding energy is exponentially small. In the other limiting case, when $a_{ex} \gg a$, we can ignore the Coulomb interaction between electrons and holes. In the interband absorption case we should observe aperiodic oscillations associated with transitions between the size quantization levels of holes and electrons.

The exciton size quantization effect was reported for CuCl microcrystals in Ref. 2 and preliminary results of an investigation of the effect were published in Ref. 3. The other limiting case of $a_{ex} \gg a$ was also studied using CdS microcrystals, which exhibited oscillations in the interband absorption spectrum due to the size quantization of the energy spectrum of free electrons.[4]

In the case when $a_{ex} \ll a$ the position of the exciton line maximum considered as a function of the average radius of microcrystals $\bar{a}$ is described by the following expression[5]:

$$\hbar\omega = E_g - E_{ex} + \hbar^2\pi^2 K/2M\bar{a}^2, \tag{1}$$

where E_g is the band gap; E_{ex} is the binding energy of an exciton; M is the translational mass of an exciton; K is a numerical coefficient governed by the size distribution of microcrystals. However, the model of a simple exciton energy band with a parabolic dispersion law considered in Ref. 5 does not describe the real band structure of CuCl crystals and gives only the first approximation to the experimental situation.

We shall report a detailed investigation of the dependences of the position and profile of the exciton luminescence and absorption lines of CuCl microcrystals on their size. We shall show that the shift and broadening of these lines are due to quantization of the energy spectrum of excitons and can be described allowing for the steady-state size distribution of microcrystals established during their growth. We shall develop a many-band theory of the size quantization effect allowing for the nonparabolicity of the exciton subband. We shall compare the experiment and theory to find the parameters of the energy band structure of CuCl crystals.

II. INVESTIGATION OF THE DISPERSION OF THE MICROCRYSTAL SIZE

Microcrystals of CuCl were grown in the interior of a silicate glass matrix to which compounds of copper and chlorine were added in concentrations of the order of 1% (Ref. 1). The microcrystals were grown by high-temperature annealing of such glasses via diffusion-type precipitation of a new phase in a supersaturated solid solution. The microcrystal size was varied deliberately by altering the annealing

 0038-5646/85/040891-07$04.00

(temperature and duration) conditions. The average microcrystal radius and the concentration of the semiconducting phase in each sample were determined by the method of low-angle x-ray scattering and the approximation of monodisperse spherical particles.[1] Since the annealing temperature was higher than the melting point of CuCl, it was natural to assume that the semiconducting phase particles were liquid during growth and spherical because of the surface tension. Therefore, we postulated that the microcrystals formed as a result of solidification of such drops were indeed near-spherical.

Samples investigated in the present study were subjected to an additional low-temperature annealing. This resulted in a considerable narrowing of the exciton line and, in the final analysis, allowed us observe directly a manifestation of the size dispersion of microcrystals in the exciton luminescence spectra of these microcrystals.

§ 1. Luminescence spectra of CuCl microcrystals

Crystals of CuCl have the cubic lattice. The valence band of these crystals is split by the spin–orbit interaction into a doubly degenerate subband Γ_7 and a quadruply degenerate subband Γ_8. In contrast to the usual diamondlike semiconductors, the Γ_7 and Γ_8 valence subbands of CuCl crystals have an inverse distribution, i.e., the doubly degenerate subband is located "above" the quadruply degenerate subband.[6] Therefore, the exciton lines observed in the luminescence spectra of these crystals are due to the annihilation of excitons associated with the simple (only spin degenerate) valence subband Γ_7.

Figure 1 shows the luminescence spectra of four samples containing microcrystals with different values of the average radius, recorded at $T = 4.2$ K. The luminescence was excited by a krypton-laser emission line ($\lambda = 356.4$ nm). It is clear from this figure that the spectra of the annealed samples containing microcrystals of sufficiently large size consisted of a narrow line with a maximum at $\hbar\omega = 3.178$ eV, which was due to the annihilation of an exciton bound to a neutral acceptor.[7] The position and width of this line were practically independent of the microcrystal size and its intensity fell rapidly on increase in the size. The luminescence spectrum included also a line due to the annihilation of free excitons. It is clear from the figure that a reduction in the microcrystal size caused this line to shift toward shorter wavelengths and, as in the case of the absorption spectra,[2,3] this was due to the quantum size effect.

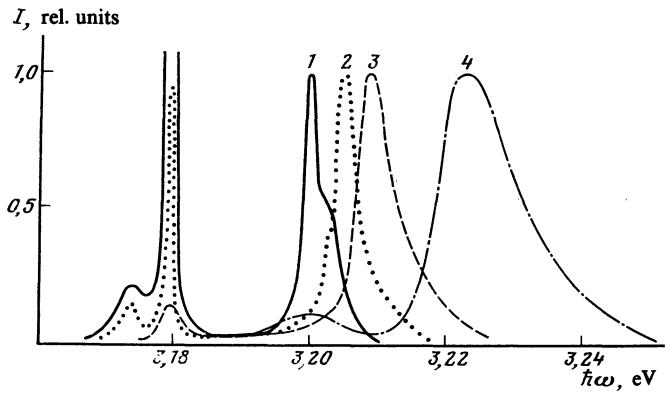

FIG. 1. Luminescence spectra of samples containing CuCl microcrystals of different radii ā (Å): 1) 140; 2) 56; 3) 45; 4) 22. $T = 4.2$ K.

The difference between the behavior of the free and bound exciton lines was due to the fact that the wave function of a bound exciton was localized near an impurity state and was insensitive to the presence of microcrystal boundaries. Therefore, the dependences of the positions of the free- and localized-exciton lines on the microcrystal size were fundamentally different.

It is also clear from the same figure that the shift of the free-exciton line was accompanied by its considerable broadening. This broadening may be due to the dispersion of the size of microcrystals and the size distribution function can be found by analyzing the profile of the exciton line. Since this line is due to the annihilation of excitons associated with the simple valence subband, the profile can be described by the size quantization theory developed in Ref. 5.

§ 2. Exciton-line profile due to the size dispersion of microcrystals

In a quantitative analysis of the experimental results on the size quantization it is necessary to know the actual form of the size distribution function of microcrystals. This is important both to allow for the influence of the size dispersion on the optical spectra [coefficient K in Eq. (1)] and to determine the average size of microcrystals from the data on low-angle x-ray scattering.

As concluded in Ref. 1, the growth of microcrystals occurred during the recondensation stage of the process of diffusion-type precipitation of a phase in a saturated solid solution when the growth of large crystals was due to the dissolution of small ones and the concentration of the semiconducting phase remained constant. This process was discussed in greater detail in the theoretical paper of Lifshitz and Slezov,[8] who found a function $P(a/\bar{a})$ describing the steady-state size distribution of the new particles which was established during recondensation growth. The explicit form of this function was used in Ref. 5 to obtain an expression for the exciton-spectrum intensity distribution resulting from the size variation of the microcrystals. An allowance for the "intrinsic" width of an exciton level made it possible to rewrite this expression as follows:

$$I(\omega) \sim \frac{1}{\pi a_{ex}^3} \cdot \frac{4}{3}\pi\bar{a}^3 \int_0^{u_0} du u^3 P(u) D\left(\hbar\omega - E_g + E_{ex} - \frac{\hbar^2\pi^2}{2M\bar{a}^2}\frac{1}{u^2}\right), \tag{2}$$

$$D(x) = \frac{1}{(2\pi)^{1/2}G}\exp\left(-\frac{x^2}{2G^2}\right),$$

where $D(x)$ is a Gaussian function describing the intrinsic width G of an exciton level and the dimensionless integration variable is $u = a/\bar{a}$.

It follows therefore that the system (2) gives the position and profile of an exciton line determined by the size quantization in the case when the size distribution of the microcrystals is governed by the Lifshitz–Slezov function. It must

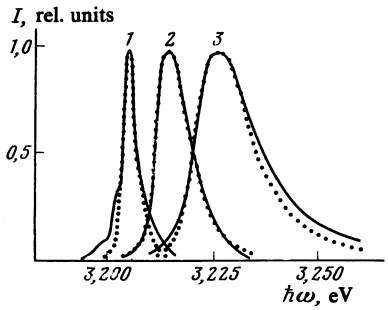

FIG. 2. Comparison of the experimental (continuous curves) and theoretical (points) profiles of the exciton luminescence lines of samples studied at $T = 4.2$ K and containing CuCl microcrystals of different radii $\bar{a}$ (Å): 1) 56; 2) 32; 3) 22.

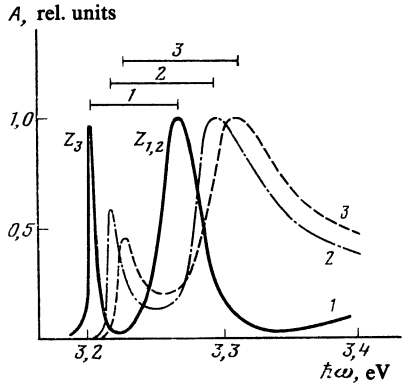

FIG. 3. Absorption spectra (here, A is the optical density) of samples containing CuCl microcrystals of different radii: 1) $\bar{a} = 270$ Å; 2) $\bar{a} = 29$ Å; 3) $\bar{a} = 22$ Å. $T = 4.2$ K.

be stressed that the only parameter that determines the size quantization of excitons in a simple parabolic energy band is their effective mass.

Experimental profiles of the free-exciton luminescence lines determined for three samples differing in respect of the average particle radius are compared in Fig. 2 with the theoretical results obtained by numerical integration of the system (2). The best agreement was obtained for the following values of the exciton mass in Eq. (2): 1) $1.9m_0$; 2) $1.9m_0$; 3) $2.0m_0$ (m_0 is the mass of a free electron). The intrinsic width G of an exciton level does not affect the position of the exciton line maximum, but governs only its long-wavelength wing. The value of G was found to be independent of the microcrystal size and in the case of the spectra shown in Fig. 2 the best agreement was obtained for the following values: 1) $G = 1.0$ meV; 2) $G = 2.5$ meV; 3) $G = 3.5$ meV. The agreement between the experimental and calculated profiles confirmed that the size distribution of microcrystals in the investigated samples was described by the Lifshitz-Slezov distribution.

It is shown in Ref. 5 that in the case of the Lifshitz–Slezov distribution the value of the coefficient K in Eq. (1) is $K = 0.67$. Moreover, since the intensity of the scattering of x rays is proportional to the square of the volume of a microcrystal, an analysis of the results of the x-ray measurements carried out in the approximation of monodisperse particles overestimated somewhat the average microcrystal radius $\bar{a}$. A numerical analysis of the results of x-ray measurements carried out allowing for the size dispersion of microcrystals showed that the average (over the Lifshitz–Slezov distribution) microcrystal radius was $\bar{a} = 0.86a$, where a is the value obtained in the monodisperse approximation. The values of the coefficients found in this way were used later in an analysis of the experimental results on the quantum size shift of exciton levels.

III. SIZE QUANTIZATION OF EXCITONS IN A COMPLEX ENERGY BAND

§ 1. Experimental results

In contrast to the luminescence spectra, we found two lines in the absorption spectra of CuCl microcrystals. The long-wavelength line Z_3 was due to the creation of excitons associated with the upper doubly degenerate valence subband Γ_7. The position of this line agreed resonantly, for all the microcrystal sizes, with the position of the free-exciton luminescence line considered in the preceding section. The short-wavelength line $Z_{1,2}$ was due to the excitation of excitons associated with the quadruply degenerate valence subband Γ_8 and the dependence of its behavior on the microcrystal size could not be described by the theory developed for a simple parabolic band.[5]

Figure 3 shows the spectra of three samples, differing in respect of the average microcrystal radius, determined at $T = 4.2$ K. Clearly, an increase in the microcrystal size resulted in a short-wavelength shift of both lines. The shift of the exciton line associated with a quadruply degenerate valence band was much stronger. We plotted in Fig. 4 (points) the positions of the maxima of both lines as a function of the reciprocal of the square of the average microcrystal radius. At high values of the radius the positions of these lines $\hbar\omega_{Z_3} = 3.201$ eV and $\hbar\omega_{Z_{1,2}} = 3.276$ eV agreed well with the published experimental data.[6] We also used the method of least squares to plot the straight lines approximating the experimental points in Fig. 4.

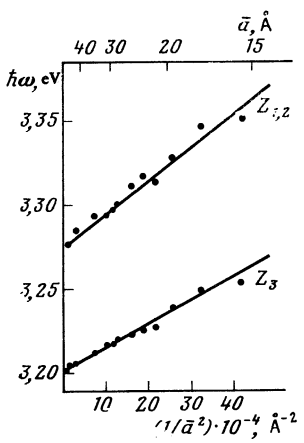

FIG. 4. Dependences of the positions of the maxima of the exciton absorption lines $Z_{1,2}$ and Z_3 at $T = 4.2$ K on the reciprocal of the square of the average radius of microcrystals.

The slope of the plot of the short-wavelength exciton-line shift associated with the upper doubly degenerate valence subband could be substituted in Eq. (1) to find, for a simple parabolic band, the effective mass of excitons which was $M = (1.9 \pm 0.2)m_0$. This value was in good agreement with the published value $M = (2.1 \pm 0.1)m_0$ (Ref. 9).

It is clear from Fig. 4 that the rate of the short-wavelength shift of the $Z_{1,2}$ line was greater than that of the Z_3 line. This was surprising because the translation mass of one of the two excitons associated with the quadruply degenerate subband was greater than for the exciton associated with the doubly degenerate subband and, consequently, the quantum size shift of the $Z_{1,2}$ line should have been less. The results obtained could be explained only by the theory of the size quantization of excitons that allowed for the real energy band structure of CuCl crystals.

§ 2. Theory

The binding energy of excitons in CuCl is 200 meV and is considerably greater than the spin–orbit splitting $\Delta = 70$ meV. The Hamiltonian describing the translation of such an exciton in the case of low momenta p, where the kinetic energy of an exciton is much less than its binding energy, may be comparable with the value of Δ:

$$\hat{H} = \frac{1}{m_0}\begin{vmatrix} \mathcal{P}+Q & L & M & 0 & i\sqrt{1/2}L & -i\sqrt{2}M \\ L^* & \mathcal{P}-Q & 0 & M & -i\sqrt{2}Q & i\sqrt{3/2}L \\ M^* & 0 & \mathcal{P}-Q & -L & -i\sqrt{3/2}L^* & -i\sqrt{2}Q \\ 0 & M^* & -L^* & \mathcal{P}+Q & -i\sqrt{2}M^* & --i\sqrt{1/2}L^* \\ -i\sqrt{1/2}L^* & i\sqrt{2}Q & i\sqrt{3/2}L & i\sqrt{2}M & \mathcal{P}-\Delta & 0 \\ i\sqrt{2}M^* & -i\sqrt{3/2}L^* & i\sqrt{2}Q & i\sqrt{1/2}L & 0 & \mathcal{P}-\Delta \end{vmatrix}, \tag{3}$$

where

$$\mathcal{P}=\gamma_1/2p^2, \quad Q=\gamma/2(p_\perp{}^2-2p_z{}^2), \quad L=-i\sqrt{3}\gamma p_- p_z,$$
$$M=\sqrt{3}/2\gamma p_-{}^2, \quad p_\perp{}^2=p_x{}^2+p_y{}^2, \quad p_-=p_x-ip_y,$$

and the energy is measured from the position of the ground state of an exciton associated with the quadruply degenerate valence subband. This Hamiltonian is written down ignoring the electron spin, exchange electron–hole interaction, and longitudinal–transverse splitting. The numerical values of the Luttinger constants γ_1 and γ (Ref. 10) describe fully the dispersion law of the ground state of an exciton in such an energy band considered in the spherical approximation. The quantities γ_1 and γ may be associated with the values of the translation masses of excitons consisting of heavy and light holes from the Γ_8 band (M_h, M_l) and a hole from the Γ_7 band (M_s):

$$M_h=m_0/(\gamma_1-2\gamma), \quad M_l=m_0/(\gamma_1+2\gamma), \quad M_s=m_0/\gamma_1. \tag{4}$$

In fact, Eq. (3) readily yields the dispersion law of an exciton in such a band:

$$E_h=(\gamma_1-2\gamma)p^2/2m_0, \tag{5a}$$

$$E_{l,s}=\frac{(\gamma_1+\gamma)}{2m_0}p^2-\frac{\Delta}{2}\pm\left[\frac{\Delta^2}{4}+\frac{\gamma p^2}{2m_0}\Delta+9\left(\frac{\gamma p^2}{2m_0}\right)^2\right]^{1/2}. \tag{5b}$$

Hence, if $\gamma p^2/m_0 \ll \Delta$, we can obtain the dispersion law of an exciton allowing for the weak nonparabolicity:

$$E_l=\frac{\gamma_1+2\gamma}{2m_0}p^2+\frac{2}{\Delta}\left(\frac{\gamma p^2}{m_0}\right)^2, \tag{6a}$$

$$E_s=\frac{\gamma_1}{2m_0}p^2-\Delta-\frac{2}{\Delta}\left(\frac{\gamma p^2}{m_0}\right)^2, \tag{6b}$$

which determines also the values of the translation masses at the bottom of the band given by Eq. (4). In the other limiting case, $\Delta \ll \gamma p^2/m_0$, we find that

$$E_l=\frac{\gamma_1+4\gamma}{2m_0}p^2-\frac{\Delta}{3}, \quad E_s=\frac{\gamma_1-2\gamma}{2m_0}p^2-\frac{2\Delta}{3}. \tag{7}$$

It is clear from Eqs. (6b) and (7) that an increase in the momentum p increases considerably the mass of an exciton formed from a hole in the spin–orbit split-off band.

A theory of the size quantization of excitons in semiconducting CuCl spheres can be developed assuming that the walls of a potential well are infinitely high at the well boundaries. Therefore, the wave function of an exciton on the surface of a well may be assumed to be zero. The wave functions of an exciton in a spherically symmetric well can be found if we begin by writing down the general form of spherically symmetric solutions of the Hamiltonian (3). In general, this can be done employing the results of Ref. 11. However, in describing our experiments it is sufficient (as shown below) to develop a theory of the size quantization in semiconductors with a quadruply degenerate valence band Γ_8. In the case of an exciton associated with the band Γ_7, a theory of its size quantization allowing for the nonparabolicity can be constructed using the Hamiltonian (3) only in the case of the states with the momentum $l = 0$, i.e., for those states which can be observed in the absorption and luminescence, in accordance with the selection rules of Ref. 5.

The Hamiltonian describing the energy spectrum of carriers at the edge of a quadruply degenerate band Γ_8 considered in the parabolic approximation can be deduced from Eq. (3) if we equate to zero the sixth and seventh columns and rows in this Hamiltonian. It is shown in Ref. 12 that spherically symmetric solutions of this Hamiltonian can be classified in accordance with the total momentum values $F = 1/2$, $3/2, \ldots$, which are all good quantum numbers. The states with a given value of F are $(2F+1)$ – fold degenerate in respect of the projection of the moment M of the vector F. The wave functions of such spherically symmetric states with given F and M are[12]

$$\psi=(2F+1)^{1/2}\sum_{l}(-1)^{l-3/2+M}R_{F,l}(r)$$
$$\sum_{m,\mu}\begin{pmatrix} l, & 3/2, & -F \\ m, & \mu, & -M\end{pmatrix} Y_{l,m}(\theta,\varphi)\chi_{\mu}, \tag{8}$$

where $Y_{l,m}(\theta,\varphi)$ are the spherical (harmonic) functions; l and m are the values of the orbital momentum and its projection; μ and χ_μ are the eigenvalues and the eigenvectors of the operator

$$J_z=\begin{pmatrix} 3/2 & 0 & 0 & 0 \\ 0 & 1/2 & 0 & 0 \\ 0 & 0 & -1/2 & 0 \\ 0 & 0 & 0 & -3/2\end{pmatrix},$$

$\begin{pmatrix} a, & b, & c \\ e, & f, & g\end{pmatrix}$ are the $3j$ Wigner symbols; $M=m+\mu$; $\mu=\pm 1/2$ and $\pm 3/2$. In the case of even (relative to the coordinate origin) solutions, the wave function for given values of F and M contains two terms with l amounting to $F+1/2$ and $F-3/2$. Using the system of equations for $R_{3/2,l}$ from Ref. 12, we can readily show that the radial wave functions of the even states of a spherically symmetric well should have the form

$$R_{F,F+1/2}=Aj_{F+1/2}(kr)+Bj_{F+1/2}(kr\beta^{1/2}),$$
$$R_{F,F-3/2}=A'j_{F-3/2}(kr)+B'j_{F-3/2}(kr\beta^{1/2}), \tag{9}$$

where j_l are the modified Bessel functions related to the Bessel functions with the half-integer argument $j_l(z)=(\pi/2z)^{1/2}J_{l+1/2}(z)$; the energy of motion is

$$E=\frac{\gamma_1-2\gamma}{2m_0}\hbar^2k^2;\quad A'=A\,\mathrm{tg}\frac{\alpha_F}{2},$$
$$B'=-B\,\mathrm{ctg}\frac{\alpha_F}{2};\quad \cos\alpha_F=\frac{2F-3}{4},$$

whereas the ratio of the masses of the light and heavy particles is $\beta=(\gamma_1-2\gamma)/(\gamma_1+2\gamma)$. The vanishing of the wave function of an exciton at the boundary of a sphere of radius a yields the following system of equations for the determination of the energy levels:

$$R_{F,F+1/2}(a)=Aj_{F+1/2}(k_{F,n}a)+Bj_{F+1/2}(k_{F,n}a\beta^{1/2})=0,$$
$$R_{F,F-1/2}(a)=A\,\mathrm{tg}\frac{\alpha_F}{2}j_{F-3/2}(k_{F,n}a)-B\,\mathrm{ctg}\frac{\alpha_F}{2}j_{F-3/2}(k_{F,n}a\beta^{1/2})=0, \tag{10}$$

which can be solved if

$$j_{F+1/2}(k_{F,n}a)j_{F-1/2}(k_{F,n}a\beta^{1/2})+\frac{6F-3}{2F+3}j_{F-3/2}(k_{F,n}a)j_{F+1/2}(k_{F,n}a\beta^{1/2})=0. \tag{11}$$

We have used here the relationship

$$\mathrm{tg}^2(\alpha_F/2)=(2F+3)/(6F-3).$$

Solving Eq. (11) for $k_{F,n}$ and then using the relationship between E and k, we can find the energy levels

$$E_{F,n}=\frac{\gamma_1-2\gamma}{2m_0}\hbar^2k_{F,n}^2, \tag{12}$$

where n is the serial number of the root of Eq. (11) for a given value of F. As in the case of a simple parabolic band, the value of $k_{F,n}$ can be represented in the form

$$k_{F,n}=\varphi_n^F/a, \tag{13}$$

where φ_n^D is the set of numerical coefficients dependent on the ratio of the masses of light and heavy quasiparticles $\beta=M_l/M_h$. In the case when $\beta=1(\gamma=0)$, the set of numbers φ_n^F is identical with the roots of the Bessel functions $\varphi_{l,n}$ (Ref. 5) (here, n is the serial number of the root of a modified Bessel function j_l with $l=F-3/2$), exactly as in the case of a simple parabolic band. If $\beta\ll 1$, we can expand the Bessel functions with small arguments as a series in Eq. (11) and this gives

$$j_{F+1/2}(\varphi_n^F)\approx-\frac{6F-3}{2F+3}\left(\frac{\varphi_n^F}{2}\right)^2\beta\frac{1}{F(F+1)}j_{F-3/2}(\varphi_n^F)\underset{\beta\to 0}{\longrightarrow}0. \tag{14}$$

Hence, it is clear that when the difference between the masses is large so that $M_l\ll M_h$, the numbers φ_n^F are again identical with the roots of a Bessel function j_l shifted in respect of the momentum l by 2, i.e., with $\varphi_{F+1/2,n}$. For small values of F and n this may increase considerably the roots of φ_n^F on reduction in β. For example, for excitons with the momentum $F=3/2$ (which are the only ones that contribute to the exciton absorption in CuCl) the first root of Eq. (11) for $F=3/2$ – $\varphi_1^{3/2}$ varies approximately from 3.14 to 5.76, i.e., it varies almost twofold.

We shall now consider how the influence of the many-band nature of the Hamiltonian (3) affects the size quantization levels of excitons associated with the valence subband Γ_7. The general form of the wave function of an exciton described by the Hamiltonian (3) in a spherically symmetric potential well is as follows for the states with the momentum $l=0$ (Ref. 11):

$$\psi=\begin{cases} R_h\begin{pmatrix} -Y_{2,-1} \\ \sqrt{2}iY_{2,0} \\ \sqrt{3}Y_{2,1} \\ -2iY_{2,2}\end{pmatrix}, \\ R_s\begin{pmatrix} Y_{0,0} \\ 0\end{pmatrix}\end{cases},$$

where $R_h(r)$ and $R_s(r)$ are the radial wave functions for which we can obtain the following system of equations if we substitute Eq. (15) into Eq. (3):

$$\left[\frac{\gamma_1+2\gamma}{2}\left(\frac{1}{r^2}\frac{\partial}{\partial r}r^2\frac{\partial}{\partial r}-\frac{6}{r^2}\right)+\varepsilon\right]R_h+\sqrt{2}\gamma\left(\frac{d}{dr}-\frac{1}{r}\right)\frac{d}{dr}R_s=0,$$
$$\sqrt{2}\gamma\left(\frac{d}{dr}+\frac{2}{r}\right)\left(\frac{d}{dr}+\frac{3}{r}\right)R_h+\left(\frac{\gamma_1}{2}\frac{1}{r^2}\frac{\partial}{\partial r}r^2\frac{\partial}{\partial r}+\varepsilon+\delta\right)R_s=0, \tag{16}$$

where $\varepsilon=m_0E/\hbar^2$, $\delta=m_0\Delta/\hbar^2$. Its solutions are the Bessel functions

$$R_h(r)=C_hj_2(kr),\quad R_s(r)=C_sj_0(kr), \tag{17}$$

and the coefficients C_h and C_s are related by the following system of equations:

$$\begin{aligned}&[\varepsilon-{}^1/_2(\gamma_1+2\gamma)k^2]C_h+\sqrt{2}\gamma k^2 C_s=0,\\&\sqrt{2}\gamma k^2 C_h+(\varepsilon+\delta-{}^1/_2\gamma_1 k^2)C_s=0.\end{aligned}\tag{18}$$

The condition for the solubility of the system (18) is given by the dispersion law of excitons, identical with Eq. (6b). On the other hand, for each value of the energy E there are two solutions of the (17) type differing in respect of k. In the energy range $-\Delta<E<0$ one of these values is imaginary and the square of the absolute value of $k_{s,h}$ is

$$\begin{aligned}k_{s,h}^2=&\frac{m_0}{\hbar^2(\gamma_1-2\gamma)(\gamma_1+4\gamma)}\,|2E(\gamma_1+\gamma)+\Delta(\gamma_1+2\gamma)\\&\pm\{[2E(\gamma_1+\gamma)+\Delta(\gamma_1-2\gamma)]^2-4E(E+\Delta)(\gamma_1-2\gamma)(\gamma_1+4\gamma)\}^{1/2}|.\end{aligned}\tag{19}$$

Then, the radial components of the wave functions of an exciton considered in this energy range are

$$\begin{aligned}R_h(r)=&C_h^s j_2(k_s r)+C_h^h I_2(k_h r),\\R_s(r)=&C_s^s j_0(k_s r)+C_s^h I_0(k_h r),\end{aligned}\tag{20}$$

where $I_l(z)$ are the modified Bessel functions with the complex argument, whereas the coefficients C_a^b are related by

$$\begin{aligned}C_h^s=&-(\varepsilon+\delta-{}^1/_2\gamma_1 k_s^2)/\sqrt{2}\gamma k_s^2 C_s^s,\\C_h^h=&-(\varepsilon+\delta+{}^1/_2\gamma_1 k_h^2)/\sqrt{2}\gamma k_h^2 C_s^h.\end{aligned}\tag{21}$$

Using next the boundary condition $R_h(a)=R_s(a)=0$, we obtain the following equation for determination of the size quantization levels:

$$\begin{aligned}&j_0(k_s a)I_2(k_h a)-j_2(k_s a)I_0(k_h a)\\&\times(\varepsilon+\delta-{}^1/_2\gamma_1 k_s^2)k_h^2/(\varepsilon+\delta+{}^1/_2\gamma_1 k_h^2)k_s^2=0.\end{aligned}\tag{22}$$

We shall consider the case of a weak nonparabolicity when $\gamma k_s^2\hbar^2/m_0\ll\Delta$. However, we have $k_h a\gg 1$ and $I_2(k_h a)/I_0(k_h a)\to 1$. Next, applying the expansion (6b), we readily obtain from Eq. (22) that

$$j_0(k_s a)=-\frac{4\hbar^2 k_s^2\gamma^2}{m_0\Delta\gamma_1}\,j_2(k_s a)=\alpha\ll 1.\tag{23}$$

We shall solve this equation by the method of successive approximations. We shall find first the root of the equation

$$j_0(k_s a)=j_0(\varphi)=0.\tag{24}$$

For the ground state this root is $\varphi^0=k_s^0 a=\pi$. Next, we obtain the correction to this root:

$$\Delta\varphi=\alpha\left(\frac{\partial j_0}{\partial\varphi}\right)_\pi^{-1}=-\frac{4\pi^2\gamma^2\hbar^2}{a^2 m_0\gamma_1\Delta}\,j_2(\pi)\left(\frac{\partial j_0}{\partial\varphi}\right)_\pi^{-1}=\frac{12\pi\gamma^2\hbar^2}{\gamma_1 m_0 a^2}\,\frac{1}{\Delta},\tag{25}$$

which gives $\Delta k_s=12\pi\gamma^2\hbar^2/\gamma_1 m_0 a^3\Delta$. Substituting the value of Δk_s into the expansion (6b), we obtain the correction to the size quantization levels of an exciton formed from a hole in the Γ_7 band and related to its nonparabolicity:

$$\begin{aligned}E\approx&-\Delta+\frac{\gamma_1\hbar^2 k_s^2}{2m_0}-\frac{2}{\Delta}\left(\frac{\gamma\hbar^2 k_s^2}{m_0}\right)^2\\\approx&-\Delta+\frac{\gamma_1\hbar^2(k_s^0)^2}{2m_0}+\gamma\frac{\hbar^2}{m_0}k_s^0\Delta k_s\\&-\frac{2}{\Delta}\left[\frac{\gamma\hbar^2(k_s^0)^2}{m_0}\right]^2=-\Delta+\frac{\gamma_1\hbar^2\pi^2}{2m_0a^2}-\frac{2}{\Delta}\left(\frac{\gamma\hbar^2\pi^2}{m_0a^2}\right)^2\left(1-\frac{6}{\pi^2}\right).\end{aligned}\tag{26}$$

Therefore, the nonparabolicity of the exciton spectrum should be manifested as a deviation from the linear dependence of the short-wavelength shift of the exciton line on $1/a^2$.

§ 3. Discussion of results

In the preceding subsection we found theoretically the quantum-size shift of the exciton lines associated with the subbands Γ_7 and Γ_8 of a semiconductor sphere of radius a, described by Eqs. (28) and (12) or (13), respectively. The experimental results agree with these formulas if we allow for the dispersion of the size of the spheres. We found experimentally (see Sec. II) that the distribution of the particle size of such heterophase systems grown by recondensation is described by the Lifshitz–Slezov function.[8] Then, allowing for the dispersion of the size of the spheres in the way it was done in Ref. 5, we can determine the dependence of the profile and positions of both exciton lines on the radius $\bar{a}$ averaged over the distribution. In the case of excitons associated with the valence subband Γ_7 the position of the line maximum is described by the expression

$$\hbar\omega_{Z_3}=E_g-E_{ex}+0.67\frac{\gamma_1\hbar^2\pi^2}{2m_0\bar{a}^2}-\frac{0.46}{\Delta}\left(\frac{\gamma\hbar^2\pi^2}{m_0\bar{a}^2}\right)^2 2\left(1-\frac{6}{\pi^2}\right).\tag{27}$$

Here, the last term proportional to $1/\bar{a}^4$ allows for the exciton spectrum nonparabolicity. We also see from Fig. 4 that the short-wavelength shift is a practically linear function of $1/\bar{a}^2$. Hence, it follows that the nonparabolicity of the excitons associated with the subband Γ_7 of CuCl is weak. Therefore, the exciton line shift is the same as for a simple parabolic energy band with an effective mass $M_s=m_0/\gamma_1$.

The position of the maximum of the exciton line associated with the valence subband Γ_8 depends as follows on $\bar{a}$:

$$\hbar\omega_{Z_{1,2}}=E_g+\Delta-E_{ex}+0.67\hbar^2\frac{\gamma_1-2\gamma}{2m_0\bar{a}^2}\,(\varphi_1^{3/2})^2.\tag{28}$$

Therefore, the short-wavelength shift of such an exciton with a fourfold degeneracy of the energy spectrum at $k=0$ is, as expected, inversely proportional to its "heavy" mass $M_h=m_0/(\gamma_1-2\gamma)$. However, the dependence on the energy band parameters includes also $\varphi_1^{3/2}$ representing the first root of Eq. (11) corresponding to $F=3/2$:

$$j_2(\varphi^{3/2})j_0(\varphi^{3/2}\beta^{1/2})+j_0(\varphi^{3/2})j_2(\varphi^{3/2}\beta^{1/2})=0.\tag{29}$$

Here, the parameter $\beta=(\gamma_1-2\gamma)/(\gamma_1+2\gamma)$ depends on the ratio γ/γ_1. Equation (29) replaces the corresponding equation $j_0(\varphi)=0$ for a simple energy band and, therefore, in the case of a complex band the value of $\varphi_1^{3/2}$ replaces the first root of the Bessel function $j_0(x)$, which is the number π in Eqs. (1) and (27).

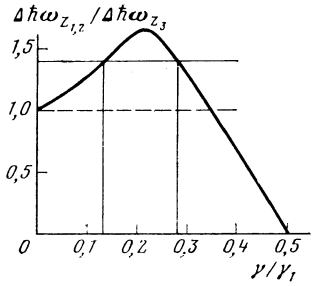

FIG. 5. Dependence of the ratio of the shifts of the exciton absorption lines $Z_{1,2}$ and Z_3 on the value of γ/γ_1.

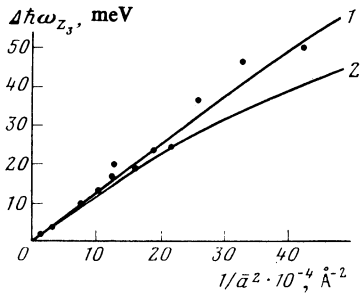

FIG. 6. Theoretical dependence of the position of the Z_3 line on the reciprocal of the square of the average radius of microcrystals, plotted allowing for the nonparabolicity of the exciton energy band. The curves correspond to different values of the parameter γ: 1) 0.07; 2) 0.15. The experimental results obtained at 4.2 K are represented by points.

In an analysis of the experimental results it is convenient to use not the absolute shift of the exciton lines

$$\Delta\hbar\omega_{Z_3}(\bar{a})=\hbar\omega_{Z_3}(a)-E_g+E_{ex},$$

$$\Delta\hbar\omega_{Z_{1,2}}(\bar{a})=\hbar\omega_{Z_{1,2}}(\bar{a})-E_g-\Delta+E_{ex},$$

but the ratio of the shifts which, in the parabolic approximation, is of the form [see Eqs. (27) and (28)]

$$\frac{\Delta\hbar\omega_{Z_{1,2}}(\bar{a})}{\Delta\hbar\omega_{Z_3}(\bar{a})}=\frac{\gamma_1-2\gamma}{\gamma_1}\left(\frac{\varphi_1^{3/2}}{\pi}\right)^2, \tag{30}$$

i.e., it is independent of the microcrystal size and is governed only by the ratio of the band parameters γ/γ_1. Figure 5 shows a theoretical plot of this dependence. We found numerically the first root $\varphi_1^{3/2}$ of Eq. (29). It is clear from this figure that the short-wavelength shift $\Delta\hbar\omega_{Z_{1,2}}$ of the excitons associated with the valence subband Γ_8 is, because of the coefficient $\varphi_1^{3/2}$, greater than $\Delta\hbar\omega_{Z_3}$ right up to $\gamma/\gamma_1\approx 0.35$. This is why the slope of the dependence $\hbar\omega_{Z_{1,2}}(\bar{a})$ in Fig. 4 is greater than that of $\hbar\omega_{Z_3}(\bar{a})$.

Figure 4 can be used to find the ratio of the short-wavelength shifts $\Delta\hbar\omega_{Z_{1,2}}/\Delta\hbar\omega_{Z_3}=1.4$. It is clear from Fig. 5 that this ratio corresponds to either $\gamma/\gamma_1=0.13$ or $\gamma/\gamma_1=0.28$. We can use the mass $M_s=1.9m_0$ of the excitons associated with the valence subband Γ_7, which corresponds to $\gamma_1=0.53$, and thus obtain two alternative values of the constant γ: $\gamma=0.07$ or $\gamma=0.15$. It is clear from Eq. (27) that the value of γ determines the degree of nonparabolicity of the exciton band associated with the Γ_7 valence subband and this makes it possible to select one of the values of γ by comparison with the experimental results. Figure 6 shows the dependences of the short-wavelength line shift Z_3 on the reciprocal of the square of the average radius of microcrystals plotted for both values of γ. We can see that $\gamma=0.07$ indeed corresponds to a weak nonparabolicity and describes better the experimental points.

The values of the Luttinger parameters $\gamma_1=0.53\pm 0.06$ and $\gamma=0.070\pm 0.007$ obtained in this way from Eq. (4) can be used to determine the translation masses of excitons. For the excitons associated with the upper valence subband Γ_7 the mass is $M_s=(1.9\pm 0.2)m_0$, in good agreement with the published data.[9] The excitons associated with the quadruply degenerate subband Γ_8 are characterized by the masses $M_h=(2.6\pm 0.2)m_0$ and $M_l=(1.5\pm(0.2)m_0$, which—to the best of our knowledge—were determined by us for the first time.

It is therefore clear that an investigation of the dependences of the positions of the exciton lines on the size of microcrystals makes it possible to study the dispersion law of excitons in a wide range of values of the quasimomentum and it provides a new method for investigating the energy band structure of semiconductor crystals.

The authors are deeply grateful to A. L. Éfros for valuable discussions.

[1]V. V. Golubkov, A. I. Ekimov, A. A. Onushchenko, and V. A. Tsekhomskiĭ, Fiz. Khim. Stekla **7**, 397 (1981).
[2]A. I. Ekimov and A. A. Onushchenko, Pis'ma Zh. Eksp. Teor. Fiz. **34**, 363 (1981). [JETP Lett. **34**, 345 (1981)].
[3]A. I. Ekimov and A. A. Onushchenko, Fiz. Tekh. Poluprovodn. **16**, 1215 (1982) [Sov. Phys. Semicond. **16**, 775 (1982)].
[4]A. I. Ekimov and A. A. Onushchenko, Trudy Vsesoyuznoĭ konferentsii po fizike poluprovodnikov (Proc. All-Union Conf. on Physics of Semiconductors), Baku, 1982, p. 176; Pis'ma Zh. Eksp. Teor. Fiz. **40**, 337 (1984) [JETP Lett. **40**, 1136 (1984)].
[5]Al. L. Éfros and A. L. Éfros, Fiz. Tekh. Poluprovodn. **16**, 1209 (1982) [Sov. Phys. Semicond. **16**, 772 (1982)].
[6]A. Goldmann, Phys. Status Solidi B **81**, 9 (1977).
[7]M. Certier, C. Wecker, and S. Nikitine, J. Phys. Chem. Solids **30**, 2135 (1969).
[8]I. M. Lifshitz and V. V. Slezov, Zh. Eksp. Teor. Fiz. **35**, 479 (1958) [Sov. Phys. JETP **8**, 331 (1959)].
[9]Y. Masumoto, Y. Unuma, Y. Tanaka, and S. Shionoya, J. Phys. Soc. Jpn. **47**, 1844 (1979).
[10]J. M. Luttinger, Phys. Rev. **102**, 1030 (1956).
[11]V. I. Sheka and D. I. Sheka, Zh. Eksp. Teor. Fiz. **51**, 1445 (1966) [Sov. Phys. JETP **24**, 975 (1967)].
[12]B. L. Gel'mont and M. I. D'yakonov, Fiz. Tekh. Poluprovodn. **5**, 2191 (1971) [Sov. Phys. Semicond. **5**, 1905 (1972)].

Translated by A. Tybulewicz